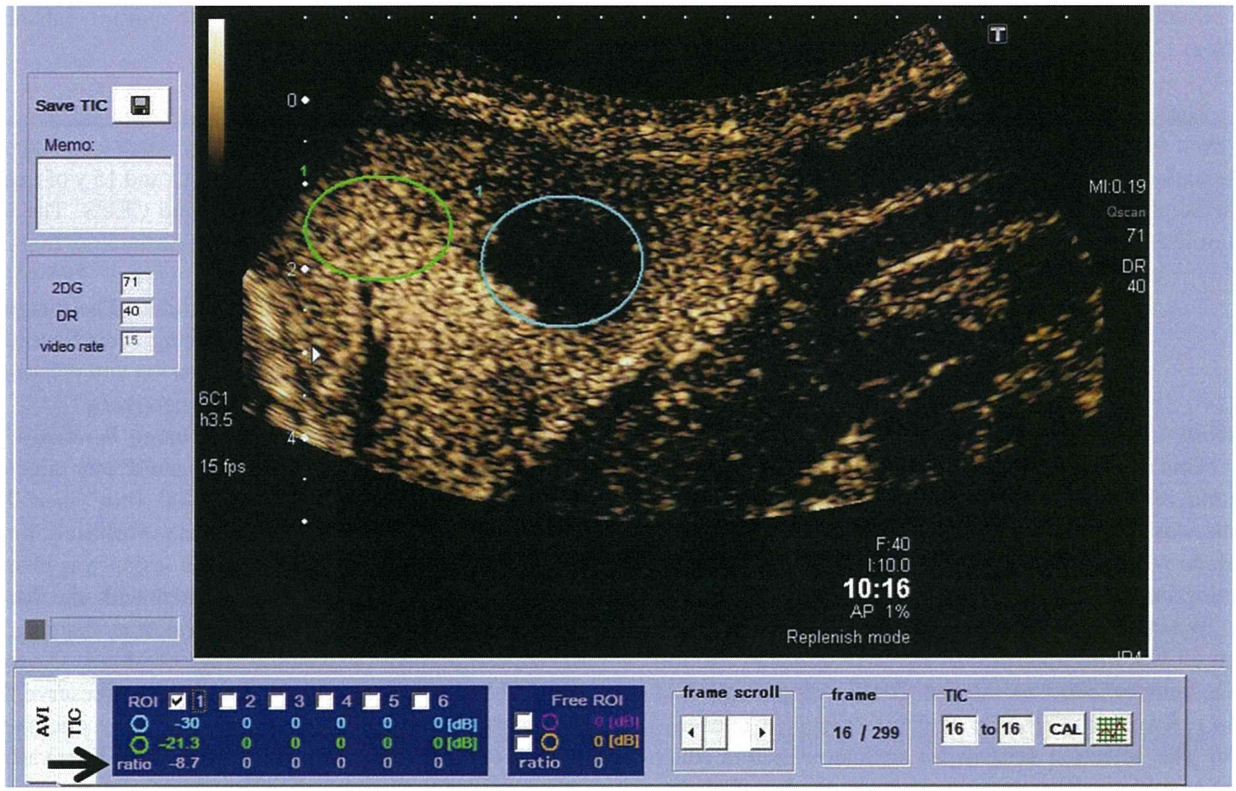

Fig. 1. Example of the software interface. A *blue* circular region of interest is placed on the hemangioma, and a *green* region of interest is placed in adjacent liver parenchyma. The contrast ratio is −8.7 dB, as illustrated in the lower part of the screen (*black arrow*).

hyper-echoic (higher echogenicity than adjacent liver parenchyma), hypo-echoic (lower echogenicity than adjacent liver parenchyma), mixed echoic (a mixture of higher and lower echogenicity within the lesion) and hyper-echoic rim (higher echogenicity at the margins of the lesion).

In the quantitative analysis, the data were analyzed using dedicated image processing software (ImageLab, Toshiba) for computing the lesion-to-liver contrast ratio in the Kupffer phase for the regions of interest (ROIs) specified in the images. An example of the software interface is illustrated in Figure 1. A ROI containing most of the lesion and a ROI containing the liver parenchyma were drawn by a radiologist (K. Saito) with 8 y of experience in US imaging. Each ROI was circular or oval, and the size of each ROI was set as large as possible while excluding large vessels. The ROI in the liver parenchyma was placed at nearly the same level as the ROI in the lesion, and the ROIs in the liver parenchyma and lesion were about the same size in each patient. The pixel values in each ROI were linearized and averaged using the inverse log-compression law of the US scanner to derive the quantitative echo power value proportional to the concentration of contrast agent (Arditi et al. 2006). Finally, for each ROI (in the lesion and liver parenchyma), the averaged echo power was obtained to calculate the lesion-to-liver contrast ratio (in decibels).

Statistical analysis

The unpaired Student *t*-test was used to identify significant differences in the lesion-to-liver contrast ratio in the Kupffer phase between typical hemangiomas and high-flow hemangiomas. All statistical analyses were performed using a computer software package (SPSS 11.0, SPSS, Tokyo, Japan). A p-value < 0.05 was considered to represent a statistically significant difference.

RESULTS

Table 1 lists mean age of the patients, number of lesions, mean diameter of the lesions and time from bolus injection of Sonazoid to determination of the lesion-to-liver contrast ratio in the Kupffer phase for patients with typical hemangiomas and those with high-flow hemangiomas separately. No significant differences were observed between patients with typical hemangiomas and those with high-flow hemangiomas with respect to any of these parameters, except number of lesions. The B-mode US findings of the typical

Table 1. Baseline characteristics of patients and lesions*

Characteristic	High-flow hemangiomas	Typical hemangiomas
Number of lesions	12	34
Age (y)	51.9 ± 16.2†	54.7 ± 13.8
Diameter of lesion (mm)	16.7 ± 6.3	20.8 ± 5.9
Timing of Kupffer phase (s)	658.9 ± 72.0	620.9 ± 56.0
B-Mode ultrasound findings		
Hyper-echoic	2	15
Hypo-echoic	3	8
Mixed echoic	2	8
Hyper-echoic rim	5	3

* There were no significant differences between the groups, except for the number of lesions.
† Mean ± standard deviation.

hemangiomas and high-flow hemangiomas are also summarized in Table 1.

Comparison between typical hemangiomas and high-flow hemangiomas in the Kupffer phase

Figures 2 and 3 are representative CEUS images of a high-flow hemangioma and a typical hemangioma, respectively. Figure 4 illustrates the lesion-to-liver contrast ratio in the Kupffer phase for the high-flow and typical hemangiomas. The contrast ratio was –5.33 ± 6.70 dB for the high-flow hemangiomas and –4.54 ± 6.28 dB for the typical hemangiomas. The contrast ratio tended to be higher for high-flow hemangiomas than for typical hemangiomas, but there was no significant difference in contrast ratio between the two types of lesions ($p = 0.73$).

Comparison between typical hemangiomas and high-flow hemangiomas, excluding hyper-echoic nodules in B-mode US, in the Kupffer phase

Figure 5 illustrates the lesion-to-liver contrast ratio in the Kupffer phase for the high-flow and typical hemangiomas, excluding hyper-echoic nodules in B-mode US because the post-contrast images obtained by pulse subtraction technology (*i.e.*, phase inversion harmonic imaging) contain not only signals from the contrast agent, but also tissue harmonic signals, especially in hyper-echoic nodules in B-mode US.

The contrast ratio was −6.05 ± 6.83 dB for the high-flow hemangiomas and −5.17 ± 6.93 dB for the typical hemangiomas. The contrast ratio also tended to be higher for high-flow hemangiomas than for typical hemangiomas, but there was no significant difference in contrast ratio between the two types of lesions ($p = 0.75$).

DISCUSSION

In our analysis of the lesion-to-liver contrast ratio in the Kupffer phase, which reflects the degree of contrast between hemangiomas and surrounding liver parenchyma, most of the hepatic hemangiomas (34 of 46 lesions, 73.9%) were found to have a negative value, indicating

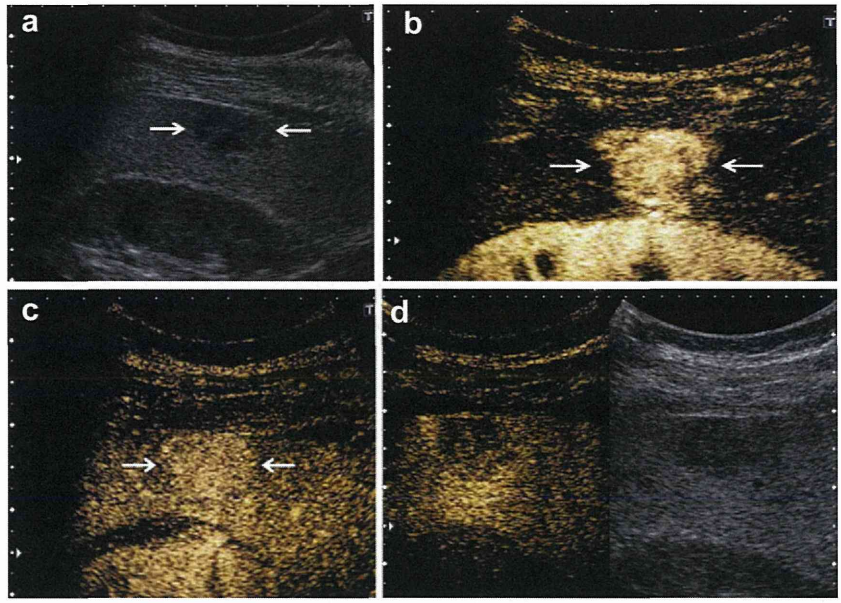

Fig. 2. Fifty-three-year-old man with normal liver function and a high-flow hemangioma in segment 6. (a) B-Mode ultrasound image reveals a hypo-echoic mass (lesion diameter = 10 mm) (*arrows*). (b) Vascular-phase image reveals homogeneous arterial enhancement of the lesion (*arrows*). (c) Late vascular-phase image reveals a slightly hyper-echoic lesion compared with adjacent liver parenchyma (*arrows*). (d) Kupffer-phase contrast image (10 min after injection) and anatomic B-mode image displayed side-by-side reveal a slightly hypo-echoic lesion compared with adjacent liver parenchyma.

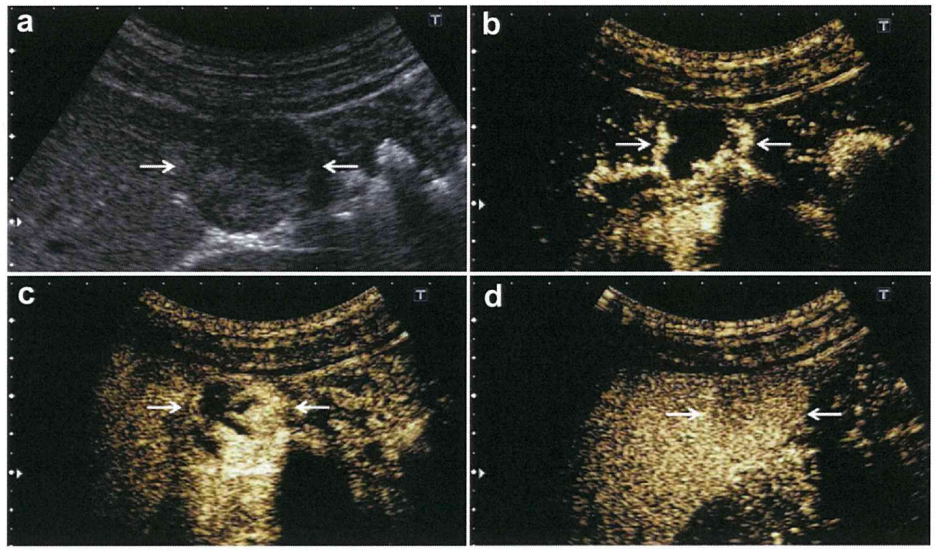

Fig. 3. Forty-six-year-old woman with normal liver function and a typical hemangioma in segment 6. (a) B-mode ultrasound image reveals a mixed-echoic mass (lesion diameter = 20 mm) (*arrows*). (b) Vascular-phase image reveals fill-in enhancement of the peripheral portion of the lesion (*arrows*). (c) Late vascular-phase image reveals nearly complete centripetal progression of fill-in enhancement (*arrows*). (d) Kupffer-phase image (10 min after injection) reveals a nearly iso-echoic lesion compared with adjacent liver parenchyma (*arrows*).

that most hemangiomas appear iso- to hypo-echoic when assessed visually. Accordingly, our results imply that vascular-phase imaging is essential for the differential diagnosis of hemangiomas and other hepatic lesions that also do not exhibit specific uptake of Sonazoid microbubbles.

The main factor responsible for the decrease in signal intensity of hepatic hemangiomas in the Kupffer phase is the increased enhancement of surrounding liver parenchyma in the Kupffer phase when Sonazoid is used. In clinical practice, on one hand, images acquired in the Kupffer phase provide essential information for the diagnosis and detection of liver tumors, especially metastatic liver tumors, because they are depicted as perfusion defects (Sugimoto et al. 2009), but on the other hand, we caution that hemangiomas may resemble other

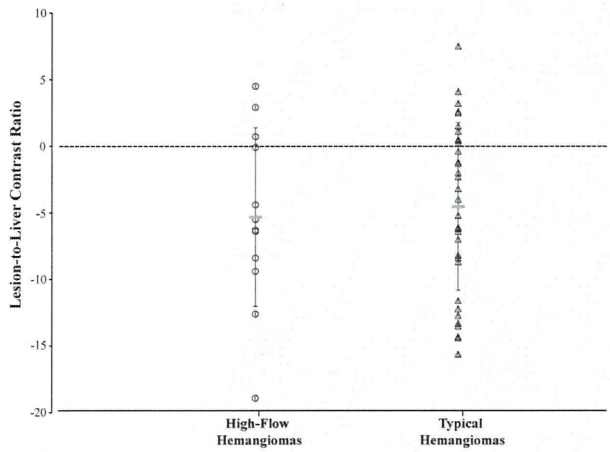

Fig. 4. Lesion-to-liver contrast ratio in the Kupffer phase for high-flow hemangiomas and typical hemangiomas. The lesion-to-liver contrast ratio in the Kupffer phase was −5.33 ± 6.70 dB for high-flow hemangiomas and −4.54 ± 6.28 dB for typical hemangiomas. The contrast ratio tended to be higher for high-flow hemangiomas than for typical hemangiomas, but there was no significant difference in contrast ratio between the two types of lesions ($p = 0.73$).

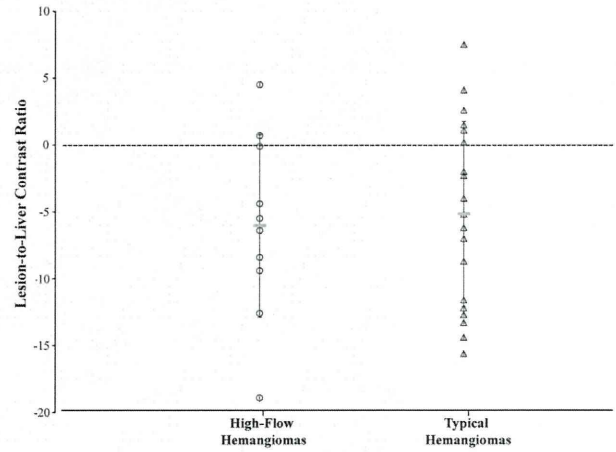

Fig. 5. Lesion-to-liver contrast ratio in the Kupffer phase for high-flow hemangiomas and typical hemangiomas, excluding hyper-echoic nodules in B-mode ultrasound. The contrast ratio was −6.05 ± 6.83 dB for high-flow hemangiomas and −5.17 ± 6.93 dB for typical hemangiomas. The contrast ratio tended to be higher for high-flow hemangiomas than for typical hemangiomas, but there was no significant difference in contrast ratio between the two types of lesions ($p = 0.75$).

hepatic lesions that also do not exhibit specific uptake of Sonazoid microbubbles, such as metastatic liver tumors and hepatocellular carcinomas.

With regard to the differences in Kupffer-phase findings between hepatic hemangiomas and other hyper-enhancing benign liver lesions such as FNH and HCAs, Hatanaka et al. (2008) reported that all of their cases of FNH (4/4) exhibited no Kupffer-phase defects (*i.e.,* iso- or hyper-enhancement). On the other hand, a case of FNH that exhibited defects in the Kupffer phase has been described (Shibasaki et al. 2008). Because the number of such nodules that have been examined is so small, it will be necessary to evaluate larger numbers of patients to clarify the characteristics of these nodules. As for HCAs, there have been no studies of Kupffer-phase findings. This may be because the incidence of HCA is low in Asian countries such as Japan and South Korea, where Sonazoid is licensed. This therefore remains an area for future research.

In the comparison of high-flow and typical hemangiomas, no significant difference was observed between the two types of hemangiomas in terms of the lesion-to-liver contrast ratio in the Kupffer phase, even though the contrast ratio tended to be higher for high-flow hemangiomas than for typical hemangiomas. On the basis of our clinical experience and another clinical study (Giannetti et al. 2013), we hypothesized that high-flow hemangiomas should have a lower accumulation of Sonazoid microbubbles than typical hemangiomas in the Kupffer phase; the mechanism of lower accumulation in hemangiomas could be arteriovenous and arteriosinusoidal shunts, which might cause the rapid elimination of contrast agent (Giannetti et al. 2013).

One possible reason that no significant differences in contrast ratio were observed between the two types of hemangiomas may be tissue harmonic signal effects; that is, the post-contrast images obtained by phase inversion harmonic technology contain not only signals from the contrast agent, but also tissue harmonic signals, especially in hyper-echoic lesions in B-mode US. Moreover, Sonazoid microbubbles require a moderate mechanical index (*e.g.,* 0.2–0.3). Tissue harmonics increase under such conditions and interfere with the contrast images acquired using Sonazoid, especially Kupffer-phase images.

To reduce these possible effects, we recalculated the ratios after excluding hyper-echoic lesions in B-mode US from both types of hemangiomas. In addition, we had previously excluded patients with underlying chronic liver disease, including fatty liver, in the selection criteria for this study. There was then little difference between the two results with and without the hyper-echoic lesions in B-mode US. We therefore think that the Kupffer-phase ratio calculated for only post-contrast images, as was done in this study, should be acceptable.

The present study suffers from some limitations. First, the number of patients was relatively small, especially with respect to high-flow hemangiomas. Another limitation is the lack of a pathologic diagnosis for all of the lesions in the study. Nevertheless, we feel that adequate imaging and clinical follow-up information was available for all of the patients, and we therefore consider our conclusions to be valid. In addition, we included only hemangiomas in the study. If we had conducted comparisons with Kupffer-phase images of other types of hepatic nodules, the argument would have been stronger. Finally, on the basis of our finding that most hepatic hemangiomas were depicted as hypo-enhancing lesions in the Kupffer phase, the differential diagnosis of hemangiomas (especially the high-flow type) and other hyper-vascular nodules such as hepatocellular carcinomas remains a critical clinical issue. However, the main purpose of the present study was to evaluate the Kupffer-phase enhancement patterns of hepatic hemangiomas in CEUS with Sonazoid. Thus, the differentiation of high-flow hemangiomas and other hyper-vascular nodules by CEUS with Sonazoid remains a topic for future investigation.

CONCLUSIONS

Most hepatic hemangiomas, whether or not they are the high-flow type, tend to exhibit iso- to hypo-intensity relative to surrounding liver parenchyma in the Kupffer phase (10 min after injection).

REFERENCES

Arditi M, Frinking PJ, Zhou X, Rognin NG. A new formalism for the quantification of tissue perfusion by the destruction-replenishment method in contrast ultrasound imaging. IEEE Trans Ultrason Ferroelectr Freq Control 2006;53:1118–1129.

Cosgrove D, Harvey C. Clinical uses of microbubbles in diagnosis and treatment. Med Biol Eng Comput 2009;47:813–826.

Dietrich CF, Mertens JC, Braden B, Schuessler G, Ott M, Ignee A. Contrast-enhanced ultrasound of histologically proven liver hemangiomas. Hepatology 2007;45:1139–1145.

Giannetti A, Franci L, Grechi C, Giangregorio F. Contrast-enhanced sonography in the diagnosis of hepatic hemangiomas: Atypical appearance due to the washout of microbubbles. J Clin Ultrasound 2013;41:361–365.

Hatanaka K, Kudo M, Minami Y, Ueda T, Tatsumi C, Kitai S, Takahashi S, Inoue T, Hagiwara S, Chung H, Ueshima K, Maekawa K. Differential diagnosis of hepatic tumors: Value of contrast-enhanced harmonic sonography using the newly developed contrast agent, Sonazoid. Intervirology 2008;51:61–69.

Kim T, Federle MP, Baron RL, Peterson MS, Kawamori Y. Discrimination of small hepatic hemangiomas from hypervascular malignant tumors smaller than 3 cm with three-phase helical CT. Radiology 2001;219:699–706.

Moriyasu F, Itoh K. Efficacy of perflubutane microbubble-enhanced ultrasound in the characterization and detection of focal liver lesions: Phase 3 multicenter clinical trial. AJR Am J Roentgenol 2009;193:86–95.

Sasaki K, Ito K, Koike S, Fujita T, Okazaki H, Matsunaga N. Differentiation between hepatic cyst and hemangioma: Additive value of breath-hold, multisection fluid-attenuated inversion-recovery magnetic resonance

imaging using half-Fourier acquisition single-shot turbo-spin-echo sequence. J Magn Reson Imaging 2005;21:29–36.
Shibasaki S, Yokoo H, Kamiyama T, Nakanishi K, Tahara M, Fukumori D, Usui A, Matsushita M, Todo S. A case of focal nodular hyperplasia difficult to diagnose preoperatively. Jpn J Gastroenterol Surg 2008;41:1692–1697.
Strobel D, Seitz K, Blank W, Schuler A, Dietrich C, von Herbay A, Friedrich-Rust M, Kunze G, Becker D, Will U, Kratzer W, Albert FW, Pachmann C, Dirks K, Strunk H, Greis C, Bernatik T. Contrast-enhanced ultrasound for the characterization of focal liver lesions: Diagnostic accuracy in clinical practice (DEGUM multicenter trial). Ultraschall Med 2008;29:499–505.
Sugimoto K, Shiraishi J, Moriyasu F, Saito K, Doi K. Improved detection of hepatic metastases with contrast-enhanced low mechanical-index pulse inversion ultrasonography during the liver-specific phase of Sonazoid: Observer performance study with JAFROC analysis. Acad Radiol 2009;16:798–809.
Yanagisawa K, Moriyasu F, Miyahara T, Yuki M, Iijima H. Phagocytosis of ultrasound contrast agent microbubbles by Kupffer cells. Ultrasound Med Biol 2007;33:318–325.

Clinical Imaging 38 (2014) 458–463

Contents lists available at ScienceDirect

Clinical Imaging

journal homepage: http://www.clinicalimaging.org

Is diffusion-weighted imaging a significant indicator of the development of vascularization in hypovascular hepatocellular lesions?☆

Kenichi Takara [a], Kazuhiro Saito [a,*], Toru Saguchi [a], Katsutoshi Sugimoto [b], Junichi Taira [b], Yasuharu Imai [b], Fuminori Moriyasu [b], Soichi Akata [a], Koichi Tokuuye [a]

[a] Department of Radiology, Tokyo Medical University
[b] Department of Gastroenterology and Hepatology, Tokyo Medical University

ARTICLE INFO

Article history:
Received 4 November 2013
Received in revised form 16 March 2014
Accepted 24 March 2014

Keywords:
Diffusion-weighted imaging
Gd-EOB-DTPA
Hepatocellular carcinoma
Hypovascular hepatocellular nodule
Development of vascularization

ABSTRACT

Objective: The objective was to evaluate the efficacy of diffusion-weighted imaging (DWI) in predicting the development of vascularization in hypovascular hepatocellular lesions (HHLs).
Materials and methods: Forty-two HHLs that were diagnosed by computed tomographic (CT) arteriography were evaluated retrospectively. The lesion on DWI was classified as isointense, hypointense, or hyperintense. Follow-up studies that included intravenous dynamic CT or magnetic resonance imaging were performed.
Results: The 730-day cumulative developments of vascularization in hypointense, isointense, and hyperintense lesions were 17%, 30%, and 40%, respectively. The differences among these developments were not statistically significant.
Conclusion: The signal intensity on DWI showed no significant difference in the development of vascularization.

1. Introduction

Hepatocellular carcinoma (HCC) develops in a multistep fashion in the following sequence: dysplastic nodule (DN); early HCC; well-differentiated HCC; nodule-in-nodule HCC; and, finally, classical hypervascular HCC [1,2]. Almost all hypervascular HCC lesions demonstrate metastasis or vascular invasion. On the other hand, hypovascular hepatocellular nodules do not demonstrate metastasis or vascular invasion; therefore, they are considered clinically benign. It is clinically advantageous to gain knowledge about the development of lesion vascularization [3].

Gadolinium-ethoxybenzyl-diethylenetriamine pentaacetic acid (Gd-EOB-DTPA; Primovist, Bayer)-enhanced magnetic resonance imaging (MRI) is a valuable imaging technique for the detection of hypovascular hepatocellular nodules [4,5].

Diffusion-weighted imaging (DWI) can determine the histological grade of differentiation in HCC [6]. Moreover, DWI is useful in distinguishing between HCC and DN [7,8]. In this study, we hypothesize that hypovascular nodules identified by DWI are more advanced and have a greater malignant potential than those which cannot be identified as such.

This study aims to retrospectively investigate whether hypovascular nodules that can be identified by DWI can predict higher development of vascularization than those that cannot be identified by DWI.

2. Materials and methods

2.1. Subjects

This retrospective study was approved by the Institutional Review Board of our institution; informed consent was waived.

Hypovascular hepatocellular nodules were identified in 51 patients with 82 nodules on Gd-EOB-DTPA-enhanced MRI after reviewing the radiological reports between January 2008 and December 2008. The coordinator was a certified radiologist with 20 years of experience. The subjects who satisfied the following inclusion criteria were enrolled in the present study: (a) nodules showed hypointensity in the hepatobiliary phase; (b) patients received computed tomographic hepatic arteriography (CTHA) within a month of performing Gd-EOB-DTPA-enhanced MRI to evaluate precise nodular arterial vascularization if the nodules showed hypovascularity; and (c) patients were observed by dynamic CT, dynamic MRI, or CTHA examinations for more than 3 months without treatment. The exclusion criteria were as follows: (a) nodules showed hypervascular foci as observed by CTHA and (b) patients with tumor invasion of the primary left and right branches or the main trunk of the portal vein. Finally, 25 patients (12 men and 13 women: mean age, 72.0; range, 48–89 years) were enrolled in the present study. The details of subject selection are shown in Fig. 1.

☆ Disclosures: The authors have no financial disclosures associated with this study.
* Corresponding author. 6-7-1 Nishishinjuku, Shinjuku-ku, Tokyo 160-0023, Japan. Tel.: +81 3 3342 6111; fax: +81 3 3348 6314.
E-mail address: saito-k@tokyo-med.ac.jp (K. Saito).

http://dx.doi.org/10.1016/j.clinimag.2014.03.013
0899-7071/

Patient selection was performed by means of a consensus reading by two radiologists, one with 20 years of experience (the coordinator) and the second with 10 years of experience. First, we confirmed the hypovascular nodules with low signal intensity in the hepatobiliary phase on Gd-EOB-DTPA-enhanced MRI and excluded cysts and liver hemangiomas based on T2-weighted imaging, DWI, and ultrasound findings. Second, intravascular arterial blood supply in hypovascular nodules was reviewed with CTHA. Hypovascular hepatocellular nodules were defined as either isodense or of low density compared with the surrounding liver parenchyma in the first phase and second phase of CTHA.

The lesions were observed between 121 and 1073 days (median, 465 days). Patients had chronic hepatitis B (2), chronic hepatitis C (20), alcoholic liver injury (2), or nonalcoholic steatohepatitis (1). The degree of cirrhosis present was classified as either Child–Pugh A (22 patients) or Child–Pugh B (3).

2.2. Magnetic resonance imaging

MR images were obtained using a 1.5-T superconductive MRI system (Avanto; Siemens, Erlangen, Germany). T1-weighted images included in-phase and opposed-phase images, and the parameters were as follows: repetition time (TR)/echo time (TE), 120/4.76, 2.38 ms; flip angle, 75°; 1 averaging; matrix, 256×140; parallel acquisition technique (PAT) factor 2 with the generalized autocalibration partially parallel acquisition (GRAPPA) algorithm; slice thickness, 6 mm; slice gap, 1.2 mm; and acquisition time, 13 s. The T2-weighted imaging parameters were as follows: TR/TE, 3600/99 ms; flip angle, 150°; echo train length, 29; matrix 256×192; slice thickness, 6 mm; 1 averaging; PAT factor 2 with the GRAPPA algorithm; and acquisition time, 14 s. DWI was performed using the respiratory trigger method [9–11]. The DWI parameters were as follows: TR/TE, 3000/71 ms; matrix, 128×128 (%); slice thickness, 6 mm; intersection gap, 1 mm; 6 signals acquired; field of view, 40 cm; 30 sections in 5–8 min; chemical shift selective method; PAT factor 2 with the GRAPPA algorithm; *b*-factor, 100 and 800 s/mm^2. The DWI motion-probing gradient pulses were placed in three orthogonal axes, and DWI was reconstructed by combining these three images. Chemical shift selective fat suppression was preferred over inversion recovery fat suppression because it yields a superior signal-to-noise ratio (SNR). Cardiac or pulse synchronization was not necessary due to the utilization of a single-shot echo-planar imaging sequence. Since low and high *b*-values are useful for detecting and characterizing benign and malignant lesions [12], we selected *b*-values of 100 and 800.

We injected Gd-EOB-DTPA (0.025 mmol/kg) at a rate of 2 ml/s via the antecubital vein followed by 40 ml of physiological saline. Dynamic study included the hepatic arterial-dominant phase, portal-dominant phase, and period 4 min after injection of the contrast material. We used a three-dimensional volumetric interpolated breath-hold examination (3D-VIBE) with the dynamic study, with the following parameters: TR/TE, 4.28/1.78 ms; flip angle, 15°; matrix 256×217; PAT factor, 2; slice thickness, 3 mm; and acquisition time, 20 s. The monitoring scan technique (Care Bolus method) was used to obtain the optimal arterial phase. The hepatobiliary phase was obtained by 3D-VIBE 20 min after injecting the contrast material.

2.3. CT hepatic arteriography

Angiography-assisted CT was performed with an angiography-combined 16-detector row CT system (Advantx ACT; GE Medical Systems, Milwaukee, WI, USA). CTHA was performed 6 s after the injection of contrast material through a catheter in the common hepatic artery or proper hepatic artery. A total of 10–30 ml of contrast material (Iomeprol 350 mg I/ml; Eisai, Tokyo, Japan) was injected at a rate of 0.8–1.5 ml/s. CTHA was carried out in three phases. Immediately after finishing the first phase, the second phase was obtained, and the third phase was obtained 2 min after beginning the injection of the contrast material. The parameters for CT acquisition were as follows: table speed, 13.7 mm/0.5 s; collimation, 10 mm; and reconstruction, 5 mm.

2.4. Follow-up study

Observation was performed with ultrasound and either intravenous dynamic CT or dynamic MRI every 3 to 4 months. Intravenous

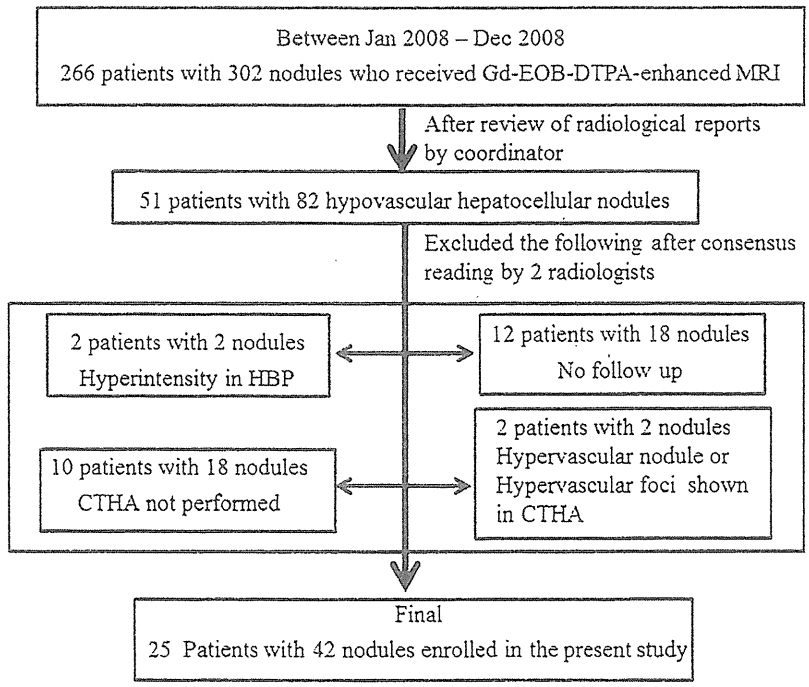

Fig. 1. The flow chart shows the patient selection process in the present study. HBP: hepatobiliary phase; CTHA: CT hepatic arteriography.

dynamic CT was performed with either a 16- or 64-detector row CT. Contrast agent was injected over 30 s [13]. The amount of contrast agent used was 600 mg I/kg [14]. The arterial-dominant phase was obtained using a monitor scan; following this, the portal-dominant phase and equilibrium phase were obtained. Dynamic MRI was performed using gadolinium-based extracellular contrast agents Gd-DTPA or Gd-EOB-DTPA. Gd-DTPA was injected at a rate of 2 ml/s via the antecubital vein followed by 40 ml of physiological saline. The total amount of contrast media used was 0.1 mmol/kg. Monitor scan was performed by first obtaining the arterial-dominant phase and then the portal-dominant and equilibrium phases.

2.5. Evaluation method

The signal intensity on DWI with the *b*-value of 800 s/mm^2[12] was evaluated by the same two radiologists mentioned previously, and lesions were classified as isointense, hypointense, or hyperintense relative to the surrounding liver parenchyma (Fig. 2). The final decisions were made by consensus. All of the follow-up studies were reviewed by the same two radiologists who recorded the incidence of vascularization. Vascularity was defined as the difference in attenuation on CT or in intensity on MRI from the surrounding liver parenchyma.

Quantitative evaluation was also performed. One certified abdominal radiologist set a region of interest (ROI) on the liver lesion and the surrounding liver parenchyma to obtain the signal intensity (SI) on DWI with a *b*-value of 800 s/mm^2. The SNR was calculated using the following formula:

$$SNR = (SI \text{ of liver lesion} - SI \text{ of liver parenchyma})/SD$$

SD refers to the standard deviation of the background noise. The background noise was measured at the ventral side of the abdominal wall. The apparent diffusion coefficient (ADC) value was measured using an ADC map. The ROI setting was taken with care. The ADC value was measured by one certified abdominal radiologist.

Analysis of variance was used for statistical analysis to compare the size of the lesions. The incidence of nonvascularization was

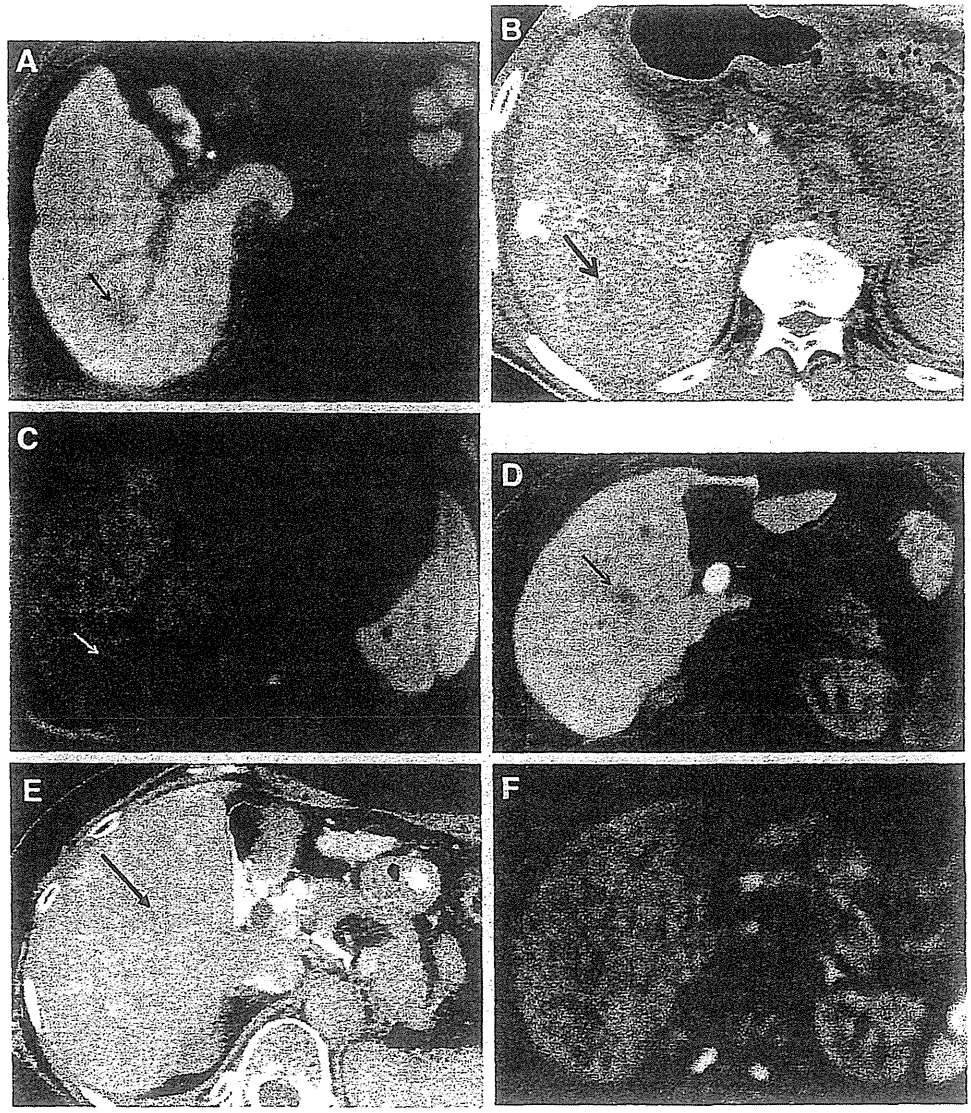

Fig. 2. (A–C) A lesion in a 73-year-old man who remained nonvascular after 429 days from the initial diagnosis. (A) Hepatobiliary phase on Gd-EOB-DTPA-enhanced MRI shows a hypointense lesion on S6 (arrow). (B) CTHA shows a low-density area on S6 (arrow). (C) DWI shows a hypointense lesion (arrow). (D–F) A lesion in a 74-year-old woman who remained nonvascular after 1073 days from the initial diagnosis. (D) Hepatobiliary phase on Gd-EOB-DTPA-enhanced MRI shows a hypointense lesion on S5 (arrow). (E) CTHA shows a low-density area on S5 (arrow). (F) DWI shows isointense lesions.

calculated using the Kaplan–Meier method, and differences were compared using the log-rank method. The incidence of vascularization ratio was calculated using the following formula: 100 minus the incidence of nonvascularization ratio (%). The Mann–Whitney test was used to evaluate the presence of significant differences between the incidence of vascularization and SNR or ADC. The Kruskal–Wallis test was used to evaluate the presence of significant differences between the qualitative classification and SNR or ADC. A two-tailed P value of less than .05 was considered to indicate a statistically significant difference. The values in the results section are described as means±standard deviation.

3. Results

The average maximum lesion dimension was 11.9±5.2 mm. Six lesions showed hypointensity, 30 lesions showed isointensity, and 6 lesions showed high signal intensity on DWI. The average maximum dimensions of the hypointense, isointense, and hyperintense lesions were 17.3±9.4, 10.7±3.8, and 12.7±2.8 mm, respectively. Only the difference in lesion size between hypointense and isointense nodules was significant. The SNRs of the hypointense, isointense, and hyperintense lesions were −13.6±7.1, −0.4±3.7, and 11.7±2.1, respectively. All of these combinations showed significant differences. The ADC value of the hypointense, isointense, and hyperintense lesions were 0.97±0.41, 1.14±0.19, and 0.99±0.18×10^{-3} mm^2/s, respectively. No significant differences were observed among all combinations.

Of the 42 nodules in 25 patients, 13 nodules (31%) in 11 patients became hypervascular during the follow-up study. The maximum dimension of the lesions which became hypervascular was 12.7±8.0 mm. The maximum dimension of the lesions which did not become hypervascular was 11.6±3.4 mm. The difference in size of lesions which became hypervascular and those that did not was not significant. The SNR of the lesion that became hypervascular was 1.7 ± 7.5. The SNR of the lesion that did not become hypervascular was −1.5±8.1. There was no significant difference between the SNRs of the lesions that became hypervascular and those of the lesions that did not become hypervascular. The ADC value of the lesion that became hypervascular was 1.15±0.13×10^{-3} mm^2/s. The ADC value of the lesion that did not become hypervascular was 1.06±0.26×10^{-3} mm^2/s. There were no significant differences between the ADC values of the lesions that became hypervascular and those of the lesions that did not become hypervascular.

The mean period in which vascularization occurred was 451±279 days (median, 429 days). One of the 6 hypointense lesions (17%), 9 of the 30 isointense lesions (33%), and 3 of the 6 hyperintense lesions (50%) became hypervascular during the follow-up period (Fig. 3). The hyperintense lesions showed the highest development of vascularization. The 730-day cumulative incidences of vascularization of hypointense, isointense, and hyperintense lesions were 17%, 30%, and 40%, respectively. The differences among the development of nonvascularization were not significant (P>.05, log-rank test) (Fig. 4).

4. Discussion

We hypothesized that the hypovascular lesions identified as hyperintense on DWI would exhibit a higher development of vascularization than those not identified as hyperintense. This was based on previous reports where such lesions showed a higher grade of malignant potential [6,8,15]. However, although these lesions had a tendency to become hypervascular, the incidence was not significant compared with lesions not identified as hyperintense on DWI. Muhi et al. reported that hypovascular lesions identified as hyperintense on DWI (b-value=1000 s/mm^2) were all poorly differentiated HCCs; therefore, DWI was useful for demonstrating the histological grade of hepatocellular lesions [15]. The hypovascular lesions, including both DNs and well-differentiated HCCs, were not identified as hyperintense on DWI, while poorly differentiated HCCs clearly showed hyperintensity on DWI. Therefore, they concluded that DWI can be used to distinguish malignant lesions among hypovascular lesions without direct evaluation of vascularity. Furthermore, Lee et al. reported that DWI was useful in distinguishing DNs and HCCs [8]. They found that

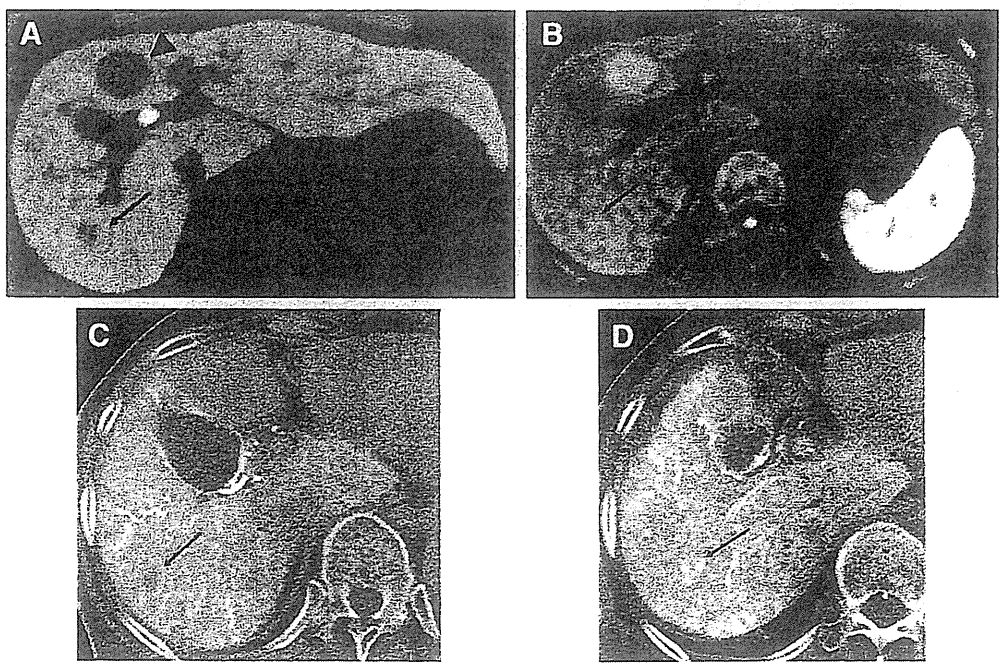

Fig. 3. (A–D) A lesion in an 82-year-old woman was found to be vascularized 827 days from the initial diagnosis. (A) Hepatobiliary phase on Gd-EOB-DTPA-enhanced MRI shows a hypointense lesion on S7 (arrow). Another hepatocellular lesion which is partially hypervascular is shown on S4 (arrowhead). (B) DWI shows a hyperintense lesion on S7 (arrow). (C) Initial CTHA from the replaced right hepatic artery shows a low-density area on S7 (arrow). Another hepatocellular lesion is fed by the middle hepatic artery. (D) CTHA from the replaced right hepatic artery after 827 days from the initial vascularity evaluation shows high density on S7 (arrow).

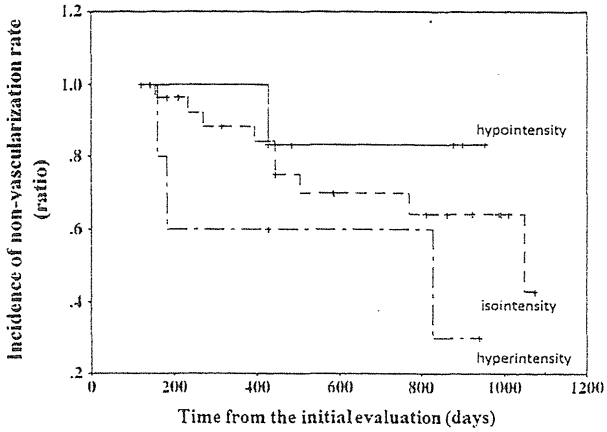

Fig. 4. Development of nonvascularization curves (calculated using the Kaplan–Meier method) for nodules categorized by DWI. The differences in the developments of nonvascularization were not significant among each of the combinations of signal intensity on DWI.

well-differentiated HCCs were mostly hypervascular; very few were hypovascular. They concluded that hypointensity in the hepatobiliary phase and hyperintensity on DWI suggested lesions which were well-differentiated HCCs rather than benign hepatocellular nodules. In the present study, all of the lesions were hypovascular, and the degree of the hyperintensity on DWI was mild to moderate; therefore, the lesions were neither poorly differentiated HCCs nor hypervascular well-differentiated HCCs. Thus, the nodules in the present study were so-called borderline lesions [16].

Xu et al. reported that almost all HCCs could be identified on DWI and 79% of dysplastic nodules showed hypointensity or isointensity on DWI [7]. In their report, it was noteworthy that 21% of dysplastic nodules showed hyperintensity. They used a lower *b*-factor ($b=500$) than we used. A low *b*-value is likely affected by the T2-shinethrough effect [17,18], and it has the potential to increase the identification of hypovascular lesions on DWI. In the present study, 6 of 42 hypovascular lesions (14%) were hyperintense on DWI; some low-grade malignant or benign hypovascular lesions exhibited hyperintensity on DWI.

It has previously been suggested that the lesion size contributes to the incidence of vascularization [19]. A diameter of ≥15 mm is associated with malignant transformation [19,20]. In the present study, the difference in size of the lesions which became hypervascular and those that did not was not statistically significant. Recently, Kim et al. also reported that the size differences were not significant between lesions which progressed to hypervascular lesions and those that did not [21]. The size of the lesions in the present study was relatively small, and this affected the results.

The cellularity of the lesion affects the signal intensity on DWI [22]. The cellularity of hypovascular well-differentiated HCCs and DNs is similar [16]. Nasu et al. reported that it was not possible to predict tumor differentiation, even roughly, using signal intensity on DWI because of overlapping among tumor grades [6]. It is presumed to be difficult to differentiate among borderline lesions when considering cellularity using DWI. However, the present study revealed that hyperintense lesions tended to have a high incidence of vascularization, although not statistically significant. Recently, Kim et al. reported similar results; however, their report showed a significantly high incidence of vascularization [21]. The initial evaluation of lesion vascularity was more precise in the present study.

Vascular endothelial growth factor (VEGF) has the potential to affect the signal intensity of the lesions on DWI [23]. VEGF, which regulates the vascular permeability and free water in the extracellular space, is increased in HCC [24]; therefore, higher VEGF expression in hypovascular hepatocellular lesions may show hyperintensity on DWI. Hypovascular well-differentiated HCC lesions that are approximately 1.0 to 1.5 cm in diameter would be in a transition stage from the portal blood supply to the arterial blood supply, which would result in an increasing VEGF expression [23,25,26]. Therefore, VEGF is one of the important factors in the case of hypovascular hyperintense lesions on DWI for inducing a high development of vascularization.

The 730-day cumulative incidence of vascularization in hyperintense lesions on DWI was higher than that in hypointense and isointense lesions, although no significant differences were noted among these groups. The incidence of vascularization in hyperintense lesions on DWI was lower than that previously reported by Hayashi et al. for partial hypervascularity and isovascularity on angiography-assisted CT [3]. They concluded that the presence of partial hypervascularity was a significant indicator for the incidence of vascularization [3]. However, the lesions with hypervascular foci were excluded from the present study by CTHA. It was considered that our patient selection process contributed towards obtaining a lower development of vascularization.

There are several limitations in the present study. Firstly, the sample size was small; a larger number of participants could have increased the significance of the findings. The sample size was determined according to those who satisfied the eligibility criteria among the consecutive patients. A larger population of hypo- and hyperintense nodules would be needed. It would however be difficult to obtain a sufficient population in a single center; therefore, a multicenter study would be needed. Secondly, histological confirmation was not obtained. This was because percutaneous biopsy increases the frequency of an arterioportal shunt near the lesion [27], making precise hemodynamic evaluation of the lesion difficult. To avoid bias, angiography-assisted CT was performed before clinical observation, and the hemodynamic quality of all lesions was examined carefully. Thirdly, the follow-up studies were performed with intravenous dynamic CT or MRI. These modalities are not sufficiently precise to evaluate vascularization when compared with CTHA. Fourthly, the injection rate of Gd-EOB-DTPA might have been so fast as to create a truncation artifact. However, the consensus report recommended the injection rate of 1–2 ml/s at the time [28]. Finally, we evaluated only the *b*-value of 800 s/mm^2. The sensitivity of detecting malignant lesions is superior at a low *b*-value on DWI, but the specificity of differentiating malignant lesions is superior at a high *b*-value on DWI [12]. Furthermore, other recent work used middle or high *b*-values to evaluate the malignant potential [7,8].

In conclusion, the signal intensity of a hypovascular hepatocellular nodule on DWI showed no significant difference in the development of vascularization.

Acknowledgments

The authors are indebted to Associate Professor Edward F. Barroga (DVM, PhD) of the Department of International Medical Communications of Tokyo Medical University for the editorial review of the English manuscript.

References

[1] Sakamoto M, Hirohashi S, Shimosato Y. Early stages of multistep hepatocarcinogenesis: adenomatous hyperplasia and early hepatocellular carcinoma. Hum Pathol 1991;22(2):172–8.
[2] Sakamoto M, Hirohashi S, Tsuda H, Shimosato Y, Makuuchi M, Hosoda Y. Multicentric independent development of hepatocellular carcinoma revealed by analysis of hepatitis B virus integration pattern. Am J Surg Pathol 1989;13(12):1064–7.
[3] Hayashi M, Matsui O, Ueda K, Kawamori Y, Gabata T, Kadoya M. Progression to hypervascular hepatocellular carcinoma: correlation with intranodular blood supply evaluated with CT during intraarterial injection of contrast material. Radiology 2002;225(1):143–9.
[4] Saito K, Kotake F, Ito N, Ozuki T, Mikami R, Abe K, Shimazaki Y. Gd-EOB-DTPA enhanced MRI for hepatocellular carcinoma: quantitative evaluation of tumor enhancement in hepatobiliary phase. Magn Reson Med Sci 2005;4(1):1–9.